In-Field and Loading Crop: A Machine Learning Approach to Classify Machine Harvesting Operating Mode

Authors: S. Harkin[1], J.T. Evans[2], Y. Zhang[2], D. Buckmaster[2], J. Krogmeier[3], D Byrne[1], M. Glavin[1]

[1] University of Galway, EEE Department, Alice Perry Engineering Building, Galway, Ireland

[2] Purdue University, ABE Department, 225 S University St, West Lafayette, IN, USA

[3] Purdue University, ECE Department, 465 Northwestern Ave, West Lafayette, IN, USA

A paper from the Proceedings of the
16th International Conference on Precision Agriculture
21-24 July 2024
Manhattan, Kansas, United States

Abstract.

Data-driven analysis can add value to the efficiency and output of modern agricultural harvesting operations. Accurate efficiency analysis and logistics planning relies on the correct classification of machinery operating modes. While rule-based methods are common within the literature, they require expertise to design and are fixed in their structure. Machine learning approaches, however, require limited prior knowledge of the machinery's operating characteristics.

In this study, RTK GPS and SAE J1939 data recorded on a combine harvester operating on a commercial farm were used to generate "harvesting" and "not-harvesting" operating mode labels. A Support Vector Machine is presented to automatically classify when the machine is harvesting, using geolocation data only. The model was trained using K-Fold cross-validation with random sampling. The model was evaluated on test data omitted during training. The results demonstrate that the best performance was achieved when using normalized speed and normalized machine heading as input features, resulting in an accuracy of 0.91.

This study demonstrates the potential of using machine learning to classify in-field machinery operating modes.

Keywords:
Operating Mode Classification, Vehicle Activity Recognition, Combine Harvester, Harvesting, Agricultural Machinery, CAN, J1939, RTK GPS

1. Introduction

Operating is identified as one of four phases in the management of agricultural machinery; it is defined as ‘executing operations using labour and machines’ (Bochtis et al., 2014). The high complexity of machine use in agricultural production means that machines have to accomplish a wide range of tasks to satisfy multiple demands (Kortenbruck et al., 2017). Jensen (2013) defined machine operating modes as the knowledge of what the machinery is doing at each time step of the operation.

Machinery operating costs constitute a significant portion of farm business expenditure (Edwards, 2015). Labelled machinery operating mode data can be used to conduct efficiency analysis (Layton et al., 2017) and influence decisions on maintenance planning (Yazdi, 2024) to ultimately reduce costs incurred by unproductive operational time. Identifying machine operating modes is critical in operational task assignment (Du et al., 2023) and scheduling (Guan et al., 2018) when multiple machinery are involved. Extensive research has been conducted on applying optimisation algorithms in production planning (Taşkıner & Bilgen, 2021) and in-field logistics, where machines must interact for shared operations (Ali et al., 2009). These methods will require accurate and automated labelling of machine operation modes to precisely reflect the current conditions (Bochtis et al., 2014).

SAE J1939 (Society of Automotive Engineers, 2024) data collected on the Controller Area Network (CAN) bus may be analyzed for operating mode classification (Kortenbruck et al., 2017) (Paraforos et al., 2017). However, acquiring and converting these data into a usable format to extract relevant features for classification requires sophisticated algorithms and data management. Alternatively, classification can be achieved by using rule-based algorithms on Global Positional System (GPS) data (Jensen & Bochtis, 2013) (Zhang et al., 2017) (Wang et al., 2023). These methods have been shown to be effective for classifying machinery operating modes. However, when designing rules, the derivation of empirical thresholds and heuristics can be particular to a specific operator, crop-type or machine. As a result, this may inhibit rule-based methods to generalize between various operation use cases.

Machine learning algorithms can remove the requirement of prior domain knowledge and programming context specific rules. Machine learning methods have been applied to classify in-field and on-road machinery data in (Poteko et al., 2021) (Chen et al., 2022). Yang (2022) reported a precision of 0.53 when using k-means clustering to classify ‘working’ and ‘turning’ operating modes for a wheat harvester operating within field boundaries. Two iterations of the k-means clustering were applied. The first iteration clusters on the relative bearing angle between points. The second round of clustering, which uses the output from the first, clusters on the distance between points. The authors reported a final precision of 0.93 after correction steps were applied to clustered output.

In this study, we define harvesting as when the machine is operating within the field boundaries and loading crop. We aim to classify samples into harvesting and not-harvesting. We use a Support Vector Machine (SVM) architecture because of its ability to transform features into a higher-dimensional space to find linearly and non-linearly separable patterns in the data (Montesinos López et al., 2022).

The main contributions of this paper are:

1. Present an SVM model to classify harvesting operating mode for a combine harvester using geolocation data only.
2. Train and evaluate the developed model using labels generated from Real-Time Kinematic (RTK) GPS and J1939 data recorded on a commercial farm.

2. Materials and Methods

2.1 Data Capture

RTK GPS and J1939 machine data were collected from a John Deere S760 combine harvester machine from a farm in West Lafayette, Indiana during 2021. The harvester worked alongside a single grain cart and two trucks to harvest corn and soybean crops (Simmons, 2024). In this study, we only considered the data collected from the harvester machine for operating mode classification. Data from the other machinery were not used.

The harvester machine RTK GPS data were sampled at 8Hz. A Kvaser Memorator Pro 2xHS logger was used to record the J1939 machine data. The logger was powered by the CAN-bus port, which automatically detected when bus traffic was active and recorded data.

In this study, we define a track as the trajectory completed by the harvester machine from when it enters the field boundaries until it exists the field boundaries. The data were segmented into tracks using manually drawn field boundaries derived from satellite images (Simmons, 2024). For a single field, there may be up to two tracks. Track samples were decimated from 8Hz to 1Hz, retaining only the first samples recorded for each second.

2.2 Data Preprocessing and Harvesting Labelling

Based on knowledge of typical machine operating patterns, it is assumed that the machine is harvesting only when moving and the header is down. Thresholds were defined for a) machine speed and b) header position data, to programmatically label the data.

a) The Haversine formula was used to calculate the distance travelled between samples. Figure 1 shows a plot of the measured speed for a track. Machine speeds greater than 0.1 m/s were labelled as ‘moving’. Moving samples were candidates for harvesting labelling.

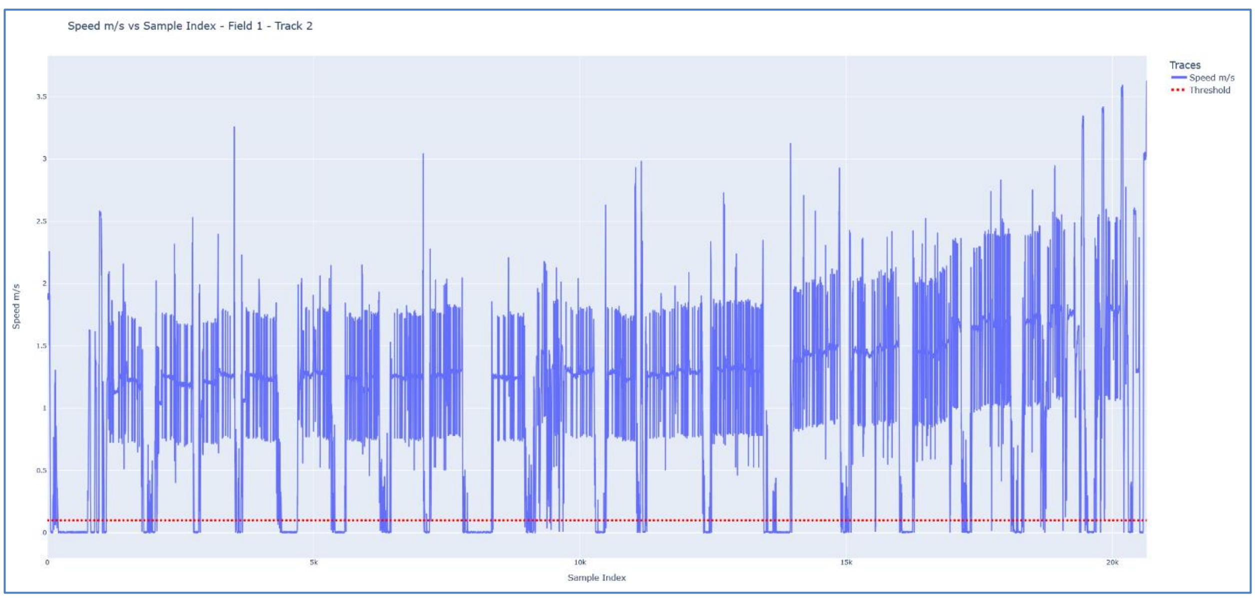

Figure 1: Plot of speed (m/s) vs sample index for Field 1 Track 2. Samples where the measured speed was greater than 0.1 m/s, represented by the dotted red line, were candidates for harvesting labelling.

b) Track header position data were decoded from an 8-bit message payload representing a value from 0 to 255. Header height can vary between fields depending on the crop condition. Therefore, for every track, header position values were plotted against sample index to determine an appropriate threshold to label the header as ‘down’. Figure 2 shows a plot of the header position for a track.

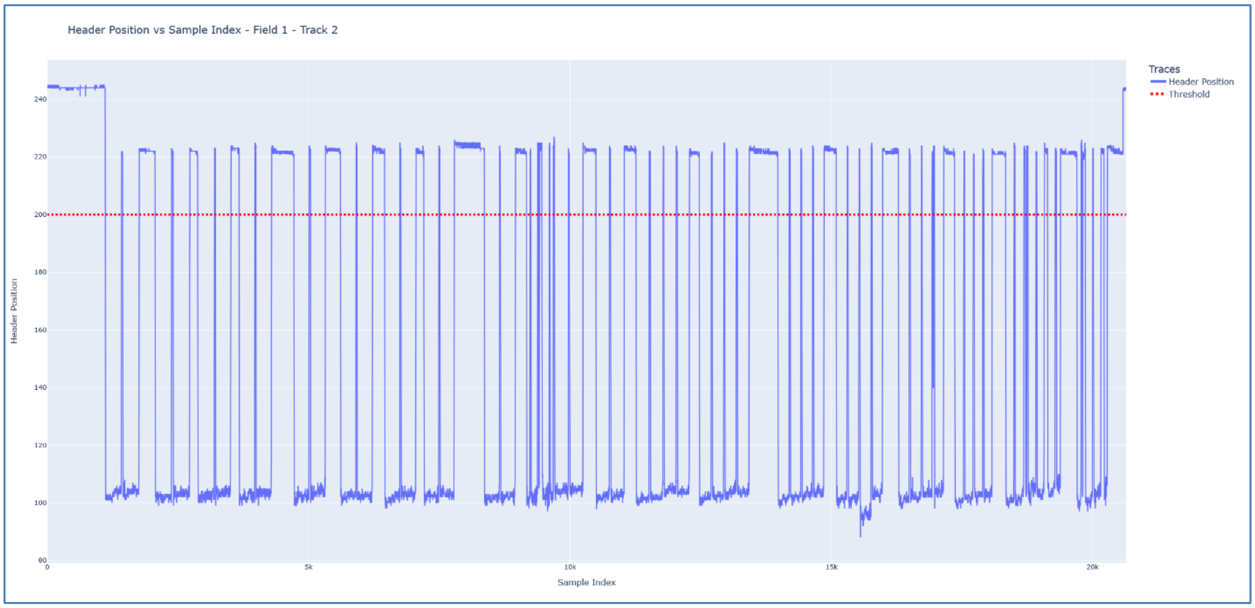

Figure 2: Plot of the header position vs sample index for Field 1 Track 2. Samples where the measured header position was less than a threshold of 200, represented by the dotted red line, were candidates for harvesting labelling.

In total, seven tracks from five fields were processed. Table 1 details the total number of harvesting samples and not-harvesting samples used for training and testing.

Table 1: Summary of the total number of samples available for training and testing. There are twice as many harvesting samples compared to not-harvesting samples in both the training and test set.

Samples	Harvesting	Not-Harvesting	Total
Training	63671	37614	101285
Test	22109	12842	34951

2.3 Feature Engineering

Machine tracks were processed individually. Three types of features were extracted per sample:

1. Machine speed
2. Machine heading
3. Latitude and longitude

Machine speed (S) was normalized (n) to the range [0,1]. For each sample, measured speed was divided by the maximum speed value recorded in the track (t). Outputs from the normalised speed were quantized into intervals of 0.05.

Machine heading (H) was calculated as the forward azimuth using the PyProj library (*Pyproj.Geod - Pyproj 3.6.1 Documentation*, 2024). This represents the angle in radians (r) measured clockwise from true north to the machine course over ground (Y_r). To convey the cyclical nature of heading to our machine learning model, cyclic encoding was performed by applying the sine transform converting the heading angle into a continuous range of [-1, 1].

Cyclic encoding was also applied to the geolocation data measurements (G). First, the latitude and longitude were converted from degrees to radians. Min-max normalization was applied to scale the data to the range [0, 2π]. Finally, the sine and cosine transforms were applied.

The features are summarized in Table 2.

Table 2: Formulae used in feature extraction from our geolocation samples for input into the model.

Feature Key	Formula	Number Of Features	Range
S	$s_n = \frac{s}{\max(s_t)}$	1	[0,1]
H	$Y_n = \sin(Y_r)$	1	[-1, 1]
G	$lat_{r\_n} = \left(\frac{lat_r - \min(lat_{t\_r})}{\max(lat_{t\_r}) - \min(lat_{t\_r})}\right) \times 2\pi, \quad lon_{r\_n} = \left(\frac{lon_r - \min(lon_{t\_r})}{\max(lon_{t\_r}) - \min(lon_{t\_r})}\right) \times 2\pi$ $\sin(lat_{r\_n}),\ \cos(lat_{r\_n}),\ \sin(lon_{r\_n}), \cos(lon_{r\_n})$	4	[-1, 1]

2.4 Training Methodology

Sci-kit Learn (*SVC*, 2024) was used to implement the SVM model architecture. To train the model, the data were split into a train and test set. One whole single track was reserved for testing to evaluate the model's performance, as shown in Table 1. Five-fold cross-validation was applied in training. Samples were randomized with a seed to ensure consistency in training.

Different combinations of the features were evaluated when training and testing the model. Two kernel functions were also evaluated, the linear kernel and the radial basis function (RBF) kernel. The linear kernel was used to determine if a linear relationship existed between the features. The RBF kernel was used to account for any non-linear relationships that may exist between features. The regularization parameter was set to '1' (default) and gamma parameter for the RBF kernel was to 'scale' (default).

3. Experimental Results

The test accuracy (AC) for each model fold is presented in Table 3. The results for recall (sensitivity), specificity, precision and F1 scores per model fold were averaged.

Table 3: Calculated metrics of model performance on the test track. Test accuracy per model fold is presented, the remaining metrics were averaged. The results show that the SVM model trained using an RBF kernel on features speed and heading produced the highest average classification accuracy at 0.91.

Kernel	Features Used	Fold 0 AC.	Fold 01 AC.	Fold 02 AC.	Fold 03 AC.	Fold 04 AC.	Fold Average Test AC.	Fold Average Sensitivity	Fold Average Specificity	Fold Average Precision	Fold Average F1 Score
Linear	All (G, S, H)	0.809	0.809	0.813	0.809	0.812	**0.81**	**0.84**	**0.76**	**0.86**	**0.85**
Linear	G, S	0.810	0.809	0.812	0.809	0.812	**0.81**	**0.84**	**0.76**	**0.86**	**0.85**
Linear	S, H	0.842	0.842	0.842	0.842	0.842	**0.84**	**0.90**	**0.74**	**0.86**	**0.88**
RBF	All (G, S, H)	0.845	0.844	0.845	0.845	0.845	**0.84**	**0.83**	**0.88**	**0.92**	**0.87**
RBF	G, S	0.862	0.863	0.862	0.862	0.862	**0.86**	**0.87**	**0.85**	**0.91**	**0.89**
RBF	S, H	0.905	0.905	0.906	0.905	0.906	**0.91**	**0.95**	**0.84**	**0.91**	**0.93**

Accuracy results on each fold show that the model was stable across all feature combinations. The linear kernel accuracy ranges from 0.81 to 0.84 and the RBF kernel accuracy ranges from 0.84 and 0.91.

The model trained using an RBF kernel on normalized speed and normalized heading returned the highest accuracy at 0.91. The model average sensitivity and average specificity were calculated at 0.95 and 0.84 respectively. These scores indicate that in general, the model performed better at predicting harvesting samples and underperformed when predicting not-harvesting samples.

Table 4 presents the model predictions for fold 0 in a confusion matrix. 20927 out of the 22109 test samples were correctly predicted as harvesting. 10709 out of the 12842 test samples were correctly predicted as not-harvesting. Figures 3, 4 and 5 are included to visualize which samples model fold 0 correctly and incorrectly classified.

Figure 3 displays a plot of the labelled test track. The machine entered the field from the top-right and navigated over to the left-hand side to begin harvesting. The machine harvested in straight-line rows, moving from left-to-right across the field. The machine performed a headland turn maneuver at the end of each harvested row to enter the next adjacent row and continue harvesting. The plot shows there was a section of unharvested ground, located in the middle-left

Table 4: Fold 0 model confusion matrix results. The total sample counts are displayed in each quadrant showing the distribution of predictions. The matrix quadrant color matches the model predictions colors used in Figures 4 and 5.

		Actual Values	
		Harvesting	NOT-Harvesting
Model Predicted Values	Harvesting	**20927** *(TP)*	**2133** *(FP)*
	NOT-Harvesting	**1182** *(FN)*	**10709** *(TN)*

hand side of the field. This area was likely not planted, possibly due to the field topography. When the operator reached this section, they encircled the unplanted ground first, and then resumed harvesting the field in a straight-line pattern.

Figure 4 displays the true positive and false positive predictions for model fold 0. Figure 4 illustrates that the model performed well in classifying straight-line harvesting samples. Additionally, the plot shows two distinct types of false positive predictions; when the machine initiated a headland turn at the end of a harvest row, and when the operator lifted the machine header in the middle of a harvest row to drive through unplanted ground.

Figure 5 displays the true negative and false negative predictions for model fold 0. The plot shows that samples at top of the field, where the machine entered the field, were correctly classified as not-harvesting. Inspecting the bottom of the plot shows that samples where the machine performed a headland turn were partly classified as not harvesting. The plot also shows that false negative predictions occur within the harvest rows.

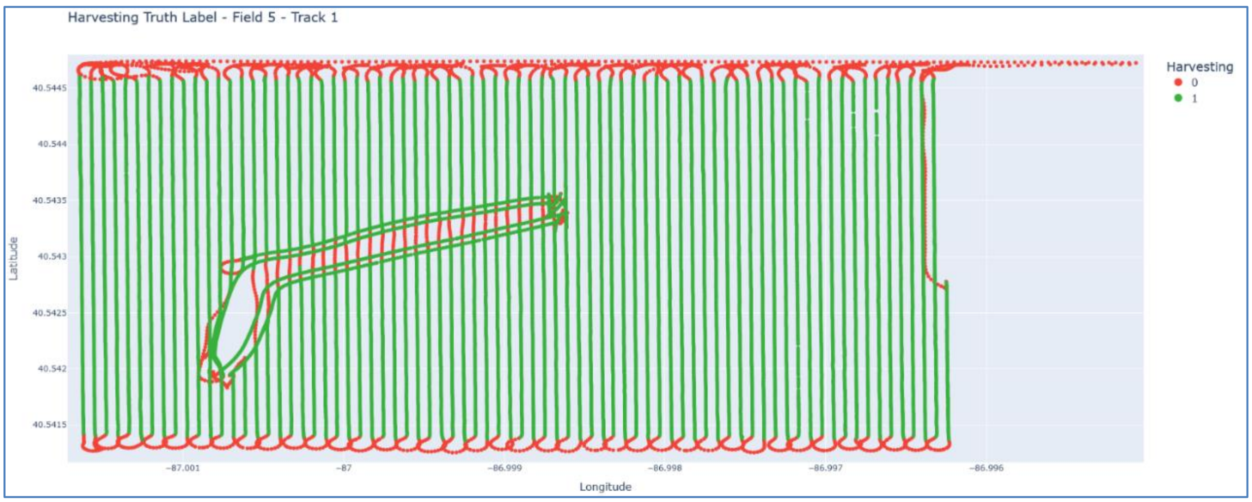

Figure 3: Labelled test track machine samples. The green colored points represent when the machine is harvesting. The red colored points represent when the machine is not harvesting. The track shows that the operator lifts the combine machine's header when navigating the headland turns and also when driving over unplanted ground.

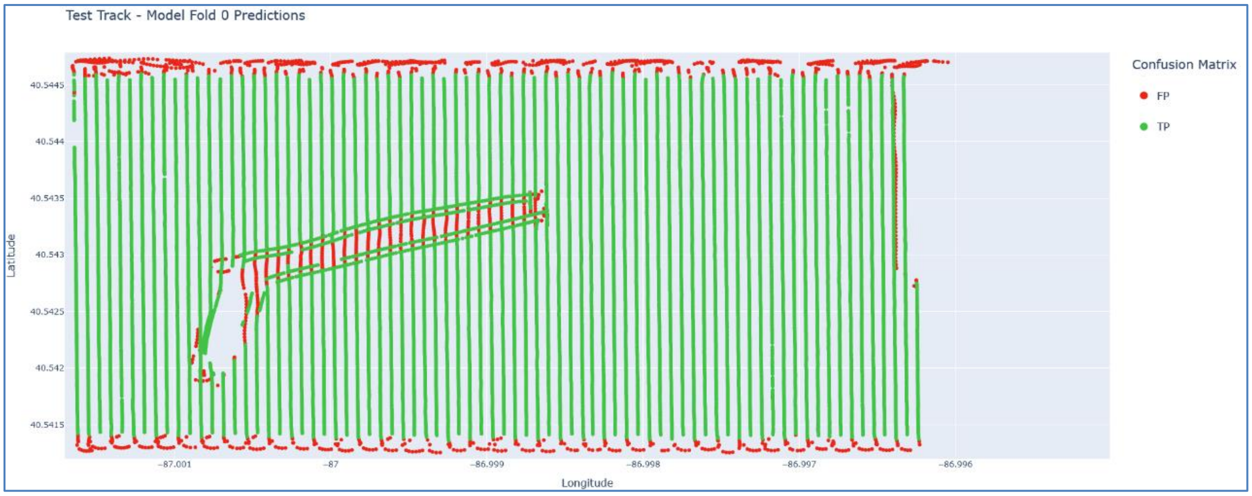

Figure 4: Fold 0 model predicted harvesting samples. The green colored points represent true positive predictions where the machine was correctly classified as harvesting. The red colored points represent false positive predictions where the machine was incorrectly classified as harvesting.

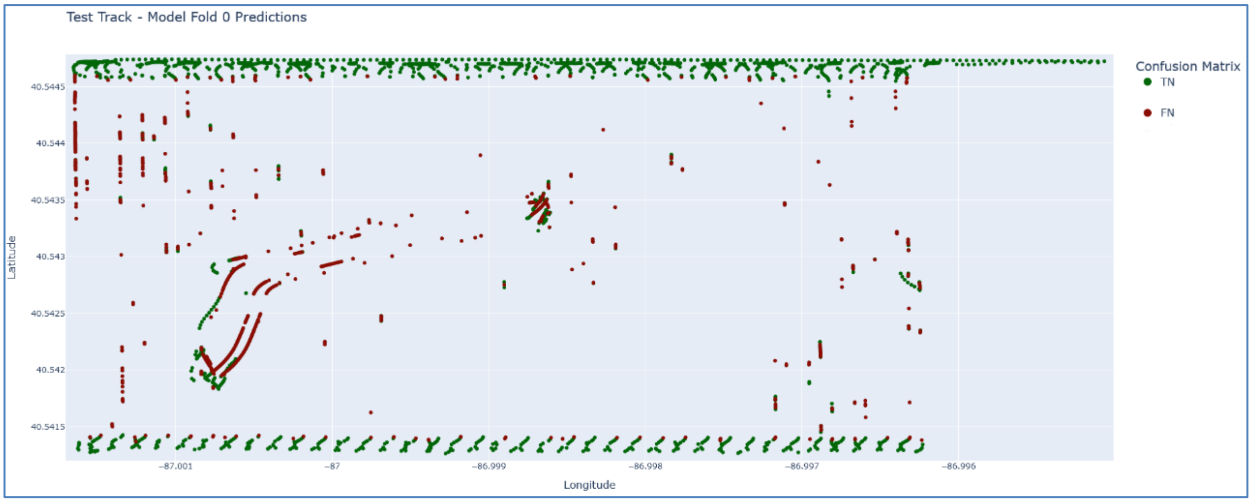

Figure 5: Fold 0 model predicted not-harvesting samples. The green colored points represent true negative predictions where the machine was correctly classified as not-harvesting. The red colored points represent false negative predictions where the machine was incorrectly classified as not-harvesting.

4. Summary

This study presents an SVM model to classify in-field combine harvester geolocation data as harvesting or not-harvesting. The model was trained and evaluated on geolocation time-series data collected from a commercial corn and soybean farm. Recorded RTK GPS and J1939 machine data were used to generate harvesting operating mode labels. K-Fold cross-validation was used in training and the model was evaluated on a track omitted during training.

The results demonstrate an accuracy of 0.91 when using the RBF kernel with normalized speed and normalized heading as input features for classification. Plots of the predicted samples show that the model was able to effectively identify straight-line harvest row samples. However, the model underperformed in classifying samples where the machine drove through unplanted ground and separately when the machine executed headland turn maneuvers.

Future work will include labelling the operation modes for other machinery involved in the harvest. We will also employ principal component analysis to inspect features for their importance and relevance. Using windowed samples, instead of individual samples, should also be investigated. Windowed samples may supply more context to the operating mode and improve classification performance.

Acknowledgments

This work is supported, in part, by the IoT4Ag project under the NSF Cooperative Agreement Number EEC-1941529. It was also funded, in part, by LERO and McHale Engineering under the SFI Grant 13/RC/2094_P2, and in part by the Enterprise Ireland Marie Skłodowska-Curie Career-FIT Fellowship under Grant MF-2018-0202.

References

Ali, O., Verlinden, B., & Van Oudheusden, D. (2009). Infield logistics planning for crop-harvesting operations. Engineering Optimization, 41(2), 183–197. https://doi.org/10.1080/03052150802406540

Bochtis, D. D., Sørensen, C. G. C., & Busato, P. (2014). Advances in agricultural machinery management: A review. Biosystems Engineering, 126, 69–81. https://doi.org/10.1016/j.biosystemseng.2014.07.012

Chen, Y., Li, G., Zhang, X., Jia, J., Zhou, K., & Wu, C. (2022). Identifying field and road modes of agricultural Machinery based on GNSS Recordings: A graph convolutional neural network approach. Computers and Electronics in Agriculture, 198, 107082. https://doi.org/10.1016/j.compag.2022.107082

Du, H. (2023). Multi-agricultural Machinery Collaborative Task Assignment Based on Improved Genetic Hybrid Optimization Algorithm (arXiv:2312.04264). arXiv. https://doi.org/10.48550/arXiv.2312.04264

Edwards, W. (n.d.). Estimating Farm Machinery Costs | Ag Decision Maker. Iowa State University Extension and Outreach. Retrieved 26 June 2024, from https://www.extension.iastate.edu/agdm/crops/html/a3-29.html

Guan, S., Shikanai, T., Nakamura, M., Fukami, K., & Takahashi, K. (2018). Practical scheduling problem for sugarcane-farming corporations and its solution. Engineering in Agriculture, Environment and Food, 11(4), 211–219. https://doi.org/10.1016/j.eaef.2018.07.002

Jensen, M. A. F., & Bochtis, D. (2013). Automatic Recognition of Operation Modes of Combines and Transport Units based on GNSS Trajectories. IFAC Proceedings Volumes, 46(18), 213–218. https://doi.org/10.3182/20130828-2-SF-3019.00059

Kortenbruck, D., Griepentrog, H. W., & Paraforos, D. S. (2017). Machine operation profiles generated from ISO 11783 communication data. Computers and Electronics in Agriculture, 140, 227–236. https://doi.org/10.1016/j.compag.2017.05.039

Layton, A. W., Zhang, Y., Krogmeier, J. V., & Buckmaster, D. R. (2017). Determining Harvesting Efficiency via Multiple Combine GPS Logs. 2017 Spokane, Washington July 16 - July 19, 2017. 2017 Spokane, Washington July 16 - July 19, 2017. https://doi.org/10.13031/aim.201700816

Montesinos López, O. A., Montesinos López, A., & Crossa, J. (2022). Support Vector Machines and Support Vector Regression. In Multivariate Statistical Machine Learning Methods for Genomic Prediction (pp. 337–378). Springer International Publishing. https://doi.org/10.1007/978-3-030-89010-0_9

Paraforos, D. S., Vassiliadis, V., Kortenbruck, D., Stamkopoulos, K., Ziogas, V., Sapounas, A. A., & Griepentrog, H. W. (2017). Multi-level automation of farm management information systems. Computers and Electronics in Agriculture, 142, 504–514. https://doi.org/10.1016/J.COMPAG.2017.11.022

Poteko, J., Eder, D., & Noack, P. O. (2021). Identifying operation modes of agricultural vehicles based on GNSS measurements. Computers and Electronics in Agriculture, 185, 106105. https://doi.org/10.1016/j.compag.2021.106105

pyproj.geod—Pyproj 3.6.1 documentation. (n.d.). Retrieved 24 June 2024, from https://pyproj4.github.io/pyproj/stable/_modules/pyproj/geod.html#Geod.inv

Simmons, C. E. C. (2024). GRAIN HARVESTING LOGISTICAL TRACKING – UTILIZING GPS DATA TO BETTER UNDERSTAND GRAIN HARVESTING EFFICIENCY [Thesis, Purdue University Graduate School]. https://doi.org/10.25394/PGS.25676307.v1

Society of Automotive Engineers. (2024). SAE J1939 Standards Collection. https://www.sae.org/publications/collections/content/j1939_dl/

SVC. (2024, June 26). Scikit-Learn. https://scikit-learn/stable/modules/generated/sklearn.svm.SVC.html

Taşkıner, T., & Bilgen, B. (2021). Optimization Models for Harvest and Production Planning in Agri-Food Supply Chain: A Systematic Review. Logistics, 5(3), 52. https://doi.org/10.3390/logistics5030052

Wang, Y., Zhang, Y., Buckmaster, D. R., & Krogmeier, J. V. (2023). A Methodology for Combine Performance Analyses in Wheat Harvests with GNSS Data. Journal of the ASABE, 66(6), 1391–1414. https://doi.org/10.13031/ja.15388

Yang, L., Wang, X., Li, Y., Xie, Z., Xu, Y., Han, R., & Wu, C. (2022). Identifying Working Trajectories of the Wheat Harvester In-Field Based on K-Means Algorithm. Agriculture, 12(11), 1837. https://doi.org/10.3390/agriculture12111837

Yazdi, M. (2024). Maintenance Strategies and Optimization Techniques. In M. Yazdi (Ed.), Advances in Computational Mathematics for Industrial System Reliability and Maintainability (pp. 43–58). Springer Nature Switzerland. https://doi.org/10.1007/978-3-031-53514-7_3

Zhang, Y., Ault, A., Krogmeier, J. V., & Buckmaster, D. (2017). Activity Recognition for Harvesting via GPS Tracks. 2017 Spokane, Washington July 16 - July 19, 2017. 2017 Spokane, Washington July 16 - July 19, 2017. https://doi.org/10.13031/aim.201700813